Eur Radiol (2006) 16: 1915–1925
DOI 10.1007/s00330-006-0248-8

Nicholas C. Gourtsoyiannis
John Grammatikakis
George Papamastorakis
John Koutroumbakis
Panos Prassopoulos
Maria Rousomoustakaki
Nickolas Papanikolaou

Imaging of small intestinal Crohn's disease: comparison between MR enteroclysis and conventional enteroclysis

Received: 14 November 2005
Revised: 9 February 2006
Accepted: 2 March 2006
Published online: 4 May 2006

N. C. Gourtsoyiannis · J. Grammatikakis · G. Papamastorakis · N. Papanikolaou (✉)
Department of Radiology,
University of Crete
Faculty of Medicine,
University Hospital of Heraklion,
P.O. Box 1352,
71110 Heraklion, Crete, Greece
e-mail: npapan@med.uoc.gr
Tel.: +30-2810-392861
Fax: +30-2810-542095

J. Koutroumbakis · M. Rousomoustakaki
Department of Gastroenterology,
University Hospital of Heraklion,
University of Crete,
Heraklion, Greece

P. Prassopoulos
Department of Radiology,
University Hospital of Alexandroupoli,
University of Thrace,
Alexandroupoli, Greece

Abstract The purpose of this study was to compare MR enteroclysis (MRE) with conventional enteroclysis (CE) in patients with small intestinal Crohn's disease. Fifty-two consecutive patients with known or suspected Crohn's disease underwent MR and conventional enteroclysis, which was considered the gold standard. Eleven imaging features, classified in three groups, mucosal, transmural and extraintestinal, were subjectively evaluated by two experienced radiologists. MRE and CE were in full agreement in revealing, localizing and estimating the length of all involved segments of the small bowel. The sensitivity of MRE for the detection of superficial ulcers, fold distortion and fold thickening was 40, 30 and 62.5%, respectively. The sensitivity of MRE for the detection of deep ulcers, cobble-stoning pattern, stenosis and prestenostic dilatation was 89.5, 92.3, 100 and 100%, respectively. Additional findings demonstrated on MRE images included fibrofatty proliferation in 15 cases and mesenteric lymphadenopathy in 19 cases. MRE strongly correlates with CE in the detection of individual lesions expressing small intestinal Crohn's disease. It provides additional information from the mesenteries; however, its capability to detect subtle lesions is still inferior to conventional enteroclysis.

Keywords Crohn's · Comparative studies–MR enteroclysis · Conventional enteroclysis

Introduction

The radiological evaluation of small bowel remains of particular importance in clinical practice, despite the advances of endoscopic techniques available, including capsule enteroscopy. Conventional enteroclysis (CE) is considered the gold standard of the radiological examination for the evaluation of patients with suspected or known Crohn's disease, as it carries a high negative predictive value and allows identification of even subtle mucosal abnormalities [1]. However, it suffers from two major disadvantages: (1) limited information regarding the extramural-mesenteric extension of the disease and (2) the radiation exposure implied for the patients [2], mostly at a young age. Recent reports suggest that MR enteroclysis (MRE) can be successfully employed for the evaluation of small bowel diseases [3–5]. The method provides three-dimensional imaging capabilities, excellent soft tissue contrast in breath-hold acquisition times and the absence of radiation exposure. Small bowel distension is achieved by intubation, while lumen opacification is based on the administration of an appropriate contrast medium [4]. MR enteroclysis is an emerging technique for small bowel (SB) imaging combining the advantages of volume challenge

with those of cross-sectional imaging [3–6]. The purpose of the current study was to compare MR enteroclysis and conventional enteroclysis on an individual lesion detection basis and to evaluate the diagnostic efficacy of MRE in patients with Crohn's disease.

Materials and methods

Patients

The study comprised 52 consecutive patients, 22 males and 30 females, with an age range of 18–57 years and a mean age of 32.15 years, who were referred for conventional and MR enteroclysis for suspected Crohn's disease (n=27) or follow-up of known Crohn's disease (n=25) proven by histology. One patient within the latter group had undergone resection 2 years prior to the examination. Informed consent was obtained by all patients while the study was approved by the local scientific review board.

MR enteroclysis

A nasojejunal catheter was placed under fluoroscopic guidance. A mean intubation fluoroscopy time of 2.5 min (range: 2.5–3.5 min) was counted using a 12-French gauge Nolan tube. Consequently, the patient was transferred to the MRI suite. An iso-osmotic water solution with polyethylene glycol and electrolytes (PEG) (KleanPrep, Norgine, Middlesex, UK) was used to opacify and distend the bowel lumen. This contrast agent exhibits biphasic properties, providing signal intensity alterations depending on the pulse sequence used, which are low on T1-weighted and high on T2-weighted images [5]. Patients were examined in the prone position, and a torso phase-array coil was used. A total amount of 1,500 to 2,000 ml of the PEG water solution was infused through the nasojejunal catheter at a rate of approximately 80 to 120 ml/min, employing a manual, MR compatible pump, with the patient lying inside the magnet. All examinations were performed on a 1.5-T MR scanner (VisionSonata, Siemens Medical Solutions, Erlangen, Germany) with a maximum gradient field strength of 40 mT/m. The following pulse sequences were used: standard scout T1-weighted FLASH, true FISP, HASTE and T1-weighted 3D VIBE (volumetric interpolated breath-hold examination) with fat saturation [7]. The most important sequence parameters are shown in Table 1. In addition, a single-shot turbo spin-echo (SSTSE) sequence, applied every 7 s, was utilized to monitor the degree of distension and the filling process of the small bowel lumen (Fig. 1). A true FISP sequence was acquired in the coronal plane using two different image sets with 12 slices and 18-s breath-hold duration for each one. Consequently, 1 mg of Glucagon (GlucaGen, Novo Nordisk, Bagsvaerd, Denmark) was intravenously administered, and a HASTE sequence was acquired in the coronal orientation. A 0.1 mmol/kg of patient weight of gadobenate dimeglumine (Multihance, Bracco, Milan, Italy) was injected and a 3D VIBE sequence with fat saturation prepulses was acquired during breath-hold in the coronal plane 75 s after intravenous contrast medium administration. Additionally, axial slices localized in the diseased segments were acquired using the true FISP sequence. A total examination time of MRE ranged from 18 to 27 min (mean value, 22.4 min; SD 6.1 min), depending on the contrast infusion time that ranged from 8 to 18 min (mean value, 12.3 min; SD 4.5 min).

Conventional enteroclysis

Following completion of MR enteroclysis, conventional small bowel enteroclysis was performed within a 3–5-h time interval. We have adopted and used the Sellink technique as our method of choice for over 25 years [1]. Using controlled infusion under gravity, a maximum amount of 1,800 ml of dilute barium suspension (20% w/v) is utilized through the nasojejunal catheter in place. A flow rate of 75–100 ml/min can be achieved by raising the plastic enema bag containing the barium suspension to approximately 1.8 m above the height of the examination table. A steady flow of contrast medium is maintained during the examination. Compression views and spot filming are used until the contrast reaches the terminal ileum.

Imaging findings evaluation

MRE and CE imaging findings were reviewed and assessed by two experienced gastrointestinal radiologists who were

Table 1 Most important sequence parameters

	SSTSE	HASTE	3D FLASH	True FISP
Scan time	7 s	21 s	20 s	19 s
Slice thickness	100–150 mm	6 mm	2.5 mm	4 mm
No. of slices	1	18	40	12
TR/TE/a	Inf/1,200 ms/180	Inf/95 ms/180	4.8 ms/1.9 ms/45	6 ms/3 ms/70
Matrix	240×256	256×256	256×512	256×256

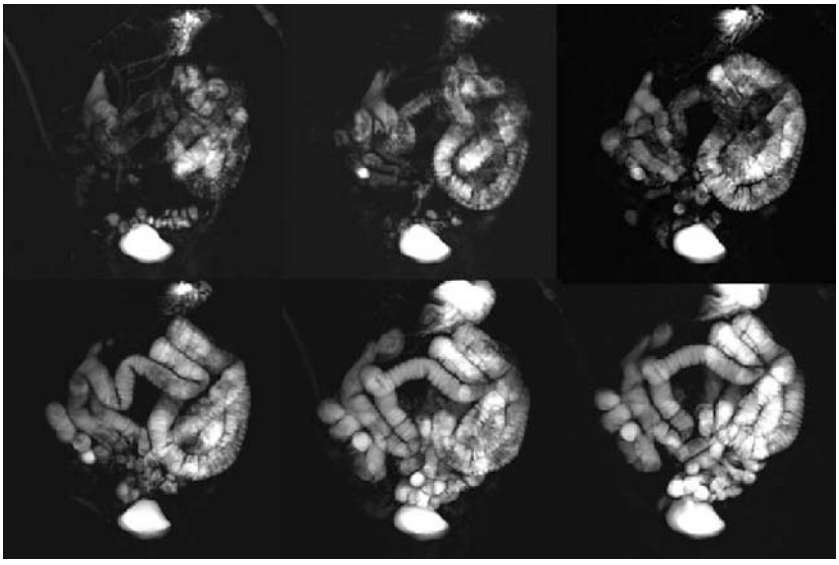

Fig. 1 Coronal SSTSE images acquired during PEG infusion through a nasojejunal catheter, showing gradual distension of bowel loops

not directly involved in performing the respective examinations, who made decisions by consensus (J.G., N.G). Both were blinded to the results of all imaging or biochemical examinations. MRE images were interpreted first, in random order; CE images were interpreted next, also in random order. The variety of imaging features seen on CE examination in patients with Crohn's disease was assessed in MRE images (Table 2) on a sign by sign basis. Receiver-operating characteristic (ROC) curves were generated, and the area under the curve for each ROC curve was calculated for each imaging sign assessed in MRE images. The sensitivity, specificity, positive predictive value (PPV) and negative predictive value (NPV) were also calculated (Table 3).

The length of the involved bowel segment(s) was estimated as short (<5 cm), medium (<5 cm and <15 cm) and long (>15 cm), and three anatomic locations were identified: the jejunum, ileum and terminal ileum. The distal ileal segment within a maximum distance of 10 cm from the ileocecal valve was defined as the terminal ileum. Three subtypes of the disease process were assessed: (1) early-minimal disease, including thickening of the valvulae conniventes, distortion of the intestinal folds and presence of superficial ulceration, (2) transmural disease, including deep ulcers, cobble-stoning, wall thickening, luminal narrowing and prestenotic dilatation and (3) extraintestinal disease, including sinus tracts, abscesses and fistula formation.

Thickening of intestinal folds was estimated by measurements greater than 2.5 mm for the jejunum and 2 mm for the ileum. Distortion of the valvulae conniventes was assessed by the absence of a normal mucosal pattern. Superficial ulcers were identified as small dots of high signal intensity surrounded by a low signal intensity rim, less than 1 cm in diameter, on true FISP images. Deep ulcers were recognized as thin, linear structures of high signal intensity, exceeding the mucosal layer, and/or penetrating the thickened bowel wall. A cobble-stoning pattern was identified as a network of high signal intensity intersecting longitudinal, transverse and/or oblique linear

Table 2 Ranking of imaging findings evaluated

	Grade 1	Grade 2	Grade 3	Grade 4
Superficial ulcers (number)	0	1	1–3	>3
Deep ulcers (number)	0	1	1–5	>5
Wall thickening	Normal <3 mm	Mild 3–5 mm	Moderate 5–10 mm	Extensive >10 mm
Sinus tract/abscess (number)	0	1	2	>2
Fistula (number)	0	1	2	>2
Stenosis–obstruction	Absent	Low-grade	High-grade	
Fold distortion	Absent	Present		
Fold thickening	Absent	Present		
Prestenotic dilatation	Absent	Present		
Cobble-stoning	Absent	Present		
Skip lesions	Absent	Present		

Table 3 Comparison results of various MRE imaging findings by considering conventional enteroclysis as a gold standard examination

Imaging sign	Sensitivity (%)	Specificity (%)	PPV (%)	NPV (%)	Area under ROC curve (95% CI)
Fold thickening	62.5	100.0	100.0	84.6	0.812 (0.675–0.909)
Fold distortion	30.0	100.0	100.0	84.8	0.650 (0.500–0.781)
Superficial ulcers	40.0	92.3	57.1	85.7	0.662 (0.512–0.790)
Deep ulcers	89.5	100.0	100.0	93.8	0.947 (0.843–0.990)
Cobble-stoning	92.3	94.4	85.7	97.1	0.934 (0.824–0.984)
Stenosis	100.0	92.9	91.3	100.0	0.964 (0.867–0.995)
Fistulae	100.0	97.8	75.0	100.0	0.989 (0.907–0.994)
Sinus tracts	100.0	100.0	100	100.0	1.000 (0.927–1.000)
Luminal dilatation	100.0	95.1	80.0	100.0	0.976 (0.885–0.997)
Skip lesions	100.0	100.0	100	100.0	1.000 (0.927–1.000)

ulcerations, surrounding residual islands of mucosa, of moderate signal intensity, on true FISP images. Sinus tracts were depicted as fissure ulcers beyond the confines of the bowel wall. Entero-enteric fistulae were recognized as thin, high-signal intensity linear structures connecting two adjacent intestinal loops.

A bowel wall thickness of 3 mm or less was considered normal. Mild thickening was noted for bowel thickness of 3–5 mm, moderate for wall thickness of 5–10 mm and extensive for wall thickness greater than 10 mm. Thickness was determined by means of visual inspection and with the use of callipers.

Abnormal bowel wall enhancement was defined as increased signal intensity on gadolinium-enhanced T1-weighted FLASH images compared with the renal cortex at visual inspection. Abnormal mural enhancement was graded as moderate when higher than that of the renal cortex and lower than that of the adjacent vessels or marked when equal to the intravascular signal enhancement. In addition, three different wall enhancement patterns were identified, as follows: (1) moderate diffuse homogeneous, exhibiting uniform mural enhancement, (2) marked homogeneous, presenting as uniform marked enhancement and (3) multi-layered, demonstrating marked enhancement of the mucosa and muscularis/serosa and lack of enhancement of the submucosa.

Luminal narrowing was identified by visual inspection, and its diameter was measured by means of callipers. Prestenotic dilation was considered when the bowel lumen proximal to the stenosis measured more than 3 cm in diameter.

Mesenteric involvement in the form of fibrofatty proliferation was only suspected on CE images and presented with space-occupying lesion characteristics, separating and/or displacing barium-filled small bowel loops. On MRE, fibrofatty proliferation was readily recognized on true FISP images as abundant bright mesenteric fat containing low signal intensity linear structures, corresponding to small mesenteric vessels. Mesenteric lymphadenopathy was additionally evaluated and recorded on MRE true FISP images as low signal intensity ovoid or round soft tissue structures within the bright mesenteric fat. Lymph nodes were classified into small, measuring less than 5 mm, medium, measuring between 5 and 10 mm, and large, measuring more than 10 mm in size.

Results

A total number of 49 involved segments in 35 patients was disclosed by MRE, all of which were confirmed by CE. There was full agreement between MRE and CE in determining the length of the diseased segments (Fig. 2). Both techniques detected 19/49 (38.7%) diseased segments less than 5 cm in length, 18/49 (36.8%) segments between 5 and 15 cm and 12/49 (24.5%) segments longer than 15 cm. Full agreement was also reached between MRE and CE in localizing the involved segment. Both techniques detected 3/49 (6.1%) jejunal diseased segments and 12/49 (24.5%) ileal diseased segments, while 34/49 (69.4%) involved segments that were located in the terminal ileum.

Early minimal disease

Thickening of intestinal folds

MRE was able to demonstrate ten segments with fold thickening (Fig. 3) and failed to detect thickening of the intestinal folds in six involved segments, resulting in a sensitivity of 62.5% and a specificity of 100% (Table 3).

Distortion of the intestinal folds

The lowest level of agreement between MRE and CE was found in the detection of distorted intestinal folds. MRE missed 7/10 (70%) segments with distortion of intestinal folds, resulting in a sensitivity of 30% and specificity of 100% (Table 3).

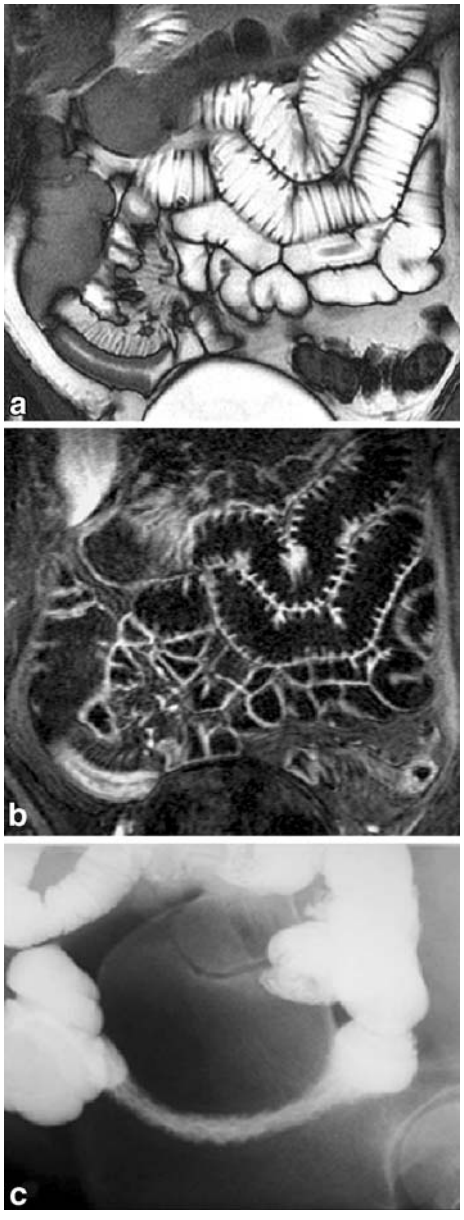

Fig. 2 Coronal (**a**) true FISP and (**b**) post-gadolinium 3D FLASH images in a patient with Crohn's disease. In (**a**) and (**b**) wall thickening is demonstrated on a distal ileal loop. (**c**) Conventional enteroclysis is in full agreement with MRE regarding the location and length of the involved segment. However, cobble-stoning appearances apparent on CE were not recognized on MRE images. Fibrofatty proliferation and the presence of lymph nodes in **a** and mucosal enhancement in **b** are additional features of MRE

Superficial ulcers

MRE detected superficial ulcers in four segments, confirmed on CE, and overlooked six segments with superficial ulcers, thus leading to a sensitivity of 40% and a specificity of 92.3% (Table 3).

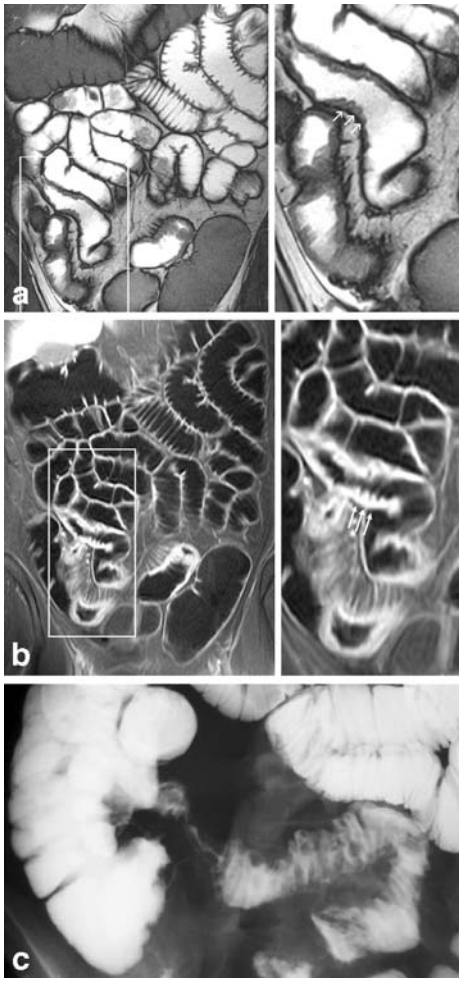

Fig. 3 Intestinal fold thickening (*arrows*) is recognized both on coronal (**a**) true FISP and (**b**) post-gadolinium 3D FLASH images in a patient with Crohn's disease, a finding that is confirmed on conventional enteroclysis (**c**)

Transmural disease

Deep ulcers

MRE detected 17/19 (89.5%) segments with deep ulcers (Fig. 4) as demonstrated on CE, resulting in a sensitivity of 89.5% and a specificity of 100% (Table 3).

Cobble-stoning appearance

MRE was able to disclose 12/13 (92.3%) segments with cobble-stoning as depicted on CE (Figs. 2 and 5). In two additional segments, the identification of cobble-stoning was not confirmed on CE. The respective sensitivity and specificity were found to be 92.3 and 94.4% (Table 3).

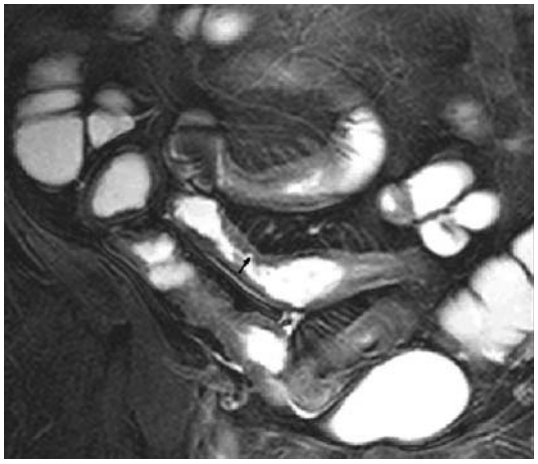

Fig. 4 Coronal true FISP image with fat saturation in a patient with Crohn's disease depicts wall thickening in three adjacent ileal loops and a small discrete ulcer (*arrow*)

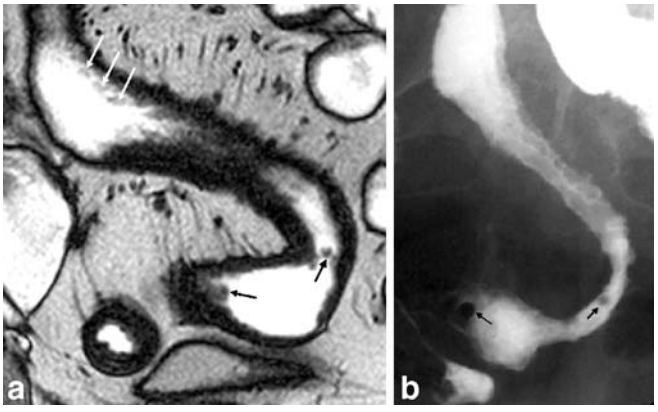

Fig. 5 Coronal true FISP spot view (**a**) in a patient with Crohn's disease demonstrates the presence of two pseudopolyps (*black arrows*), wall thickening and cobble-stoning (*white arrows*). Conventional enteroclysis spot view (**b**) is in full agreement with MRE findings

Stenosis-prestenotic dilatation

Twenty-three stenotic segments were identified on MRE images, while 21 of them were confirmed on CE, yielding a sensitivity of 100% and a specificity of 92.9% (Figs. 2, 5, 6 and 7). Prestenotic dilatation was disclosed in 10 out of 21 stenotic segments by MRE, while 8/10 (80%) were only confirmed on CE, resulting in a sensitivity of 100% and specificity of 95.1% (Table 3).

Skip lesions

Three patients out of 35 presented with skip lesions on CE, all of which were correctly identified by MRE (Fig. 8), yielding a sensitivity and specificity of 100% (Table 3).

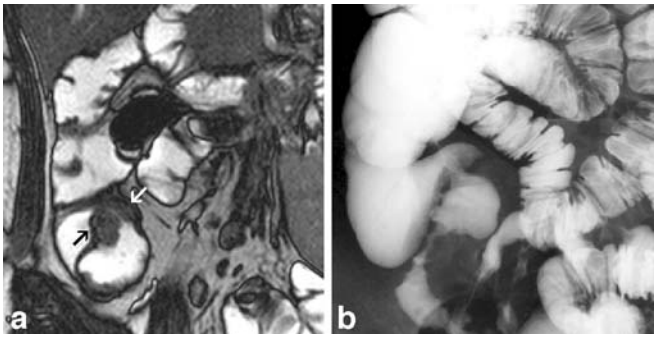

Fig. 6 Stenosis in the terminal ileum (*arrows*) and prestenotic dilatation are demonstrated equally well both on a coronal true FISP image (**a**) and conventional enteroclysis (**b**)

Extraintestinal complications: fistulae and sinus tracts formation

MRE detected four sinus tracts, all confirmed on CE, resulting in a sensitivity and specificity of 100%. Three entero-enteric fistulae were depicted on MRE images and confirmed on CE images; however, one enterocutaneous fistula was only detected by MRE (Fig. 9), resulting in a sensitivity of 100% and a specificity of 97.8% (Table 3).

Additional imaging findings

Wall thickening

MRE disclosed mild, moderate and extensive wall thickening in 14/49 (28.5%), 25/49 (51%) and 10/49 (20.5%) segments, respectively (Fig. 10). Wall thickening was suspected by CE in 38/49 (77.5%) segments. In the remaining 11 segments, CE was inconclusive for the presence of wall thickening. Thirty out of 49 segments presented with homogeneous gadolinium enhancement (Fig. 11), which was moderate in 20/30 cases and marked in 10/30 cases. A multi-layered enhancement pattern was found in 19/49 cases, featuring a high signal intensity inner layer representing mucosal hyperemia, a low signal intensity middle layer corresponding to submucosal edema and/or fat deposition and a high signal intensity outer layer representing mascularis and serosa.

Mesenteric lymph nodes

Seventy mesenteric lymph nodes were depicted in 19 patients on true FISP images. Twenty-two lymph nodes (2 small, 13 medium and 7 large in size) were surrounding the superior mesenteric artery, proximally to the origin of the ileocolic artery. Three lymph nodes (one medium and two large in size) were found around the proximal segment of the right colic artery, while 19 lymph nodes (12 medium and 7 large in size) were dispersed along the ileocolic artery

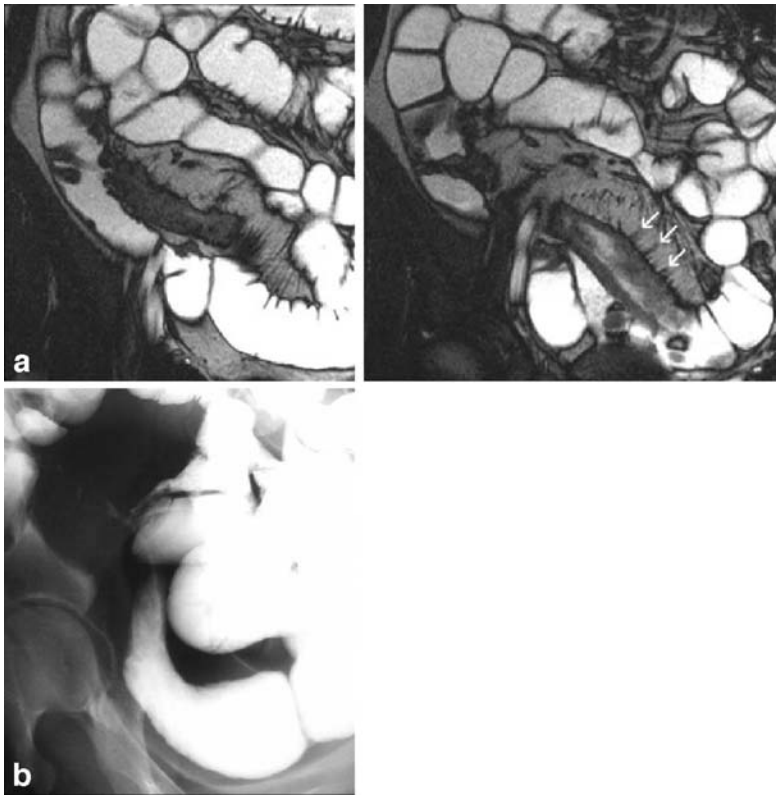

Fig. 7 Coronal true FISP successive images demonstrate the presence of a tight stenotic lesion (**a**) in the terminal ileum in a patient with Crohn's disease, confirmed by conventional enteroclysis (**b**). Additional findings revealed by true FISP image include fibrofatty proliferation and increased mesenteric vascularity at the site of involvement (*arrows*)

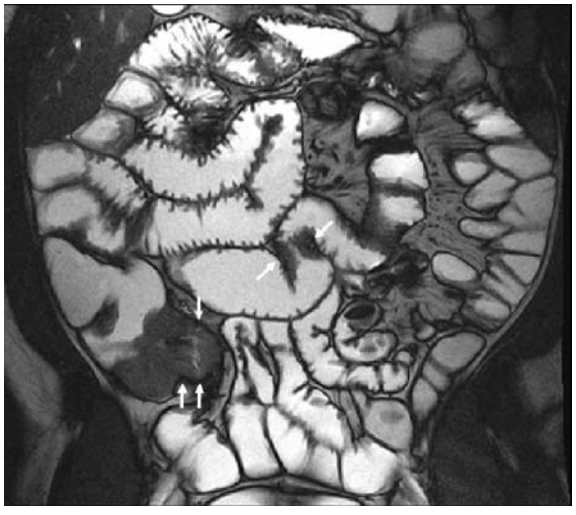

Fig. 8 Coronal true FISP image on a patient with Crohn's disease demonstrating characteristic skip lesions (*arrows*)

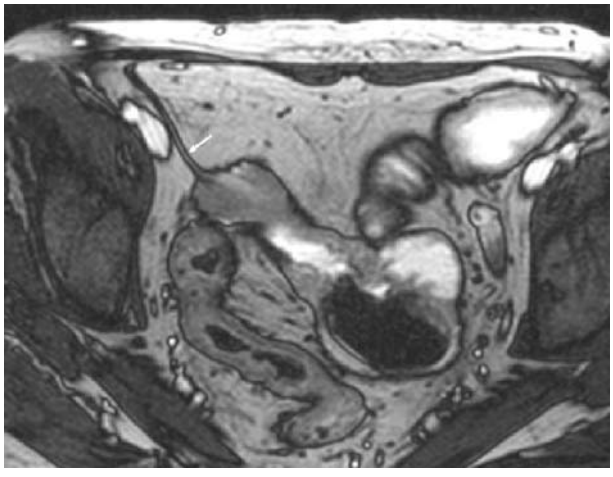

Fig. 9 Enterocutaneous fistula (*arrow*) nicely demonstrated on an axial true FISP view

(Figs. 12, 13 and 14). Twenty-one lymph nodes (13 small, 6 medium and 2 large in size) were localized across the ileal branches while 5, small in size, were found to accompany the sigmoid artery.

Fibrofatty proliferation

Fibrofatty proliferation, featuring as a blank space separating adjacent barium-filled small bowel loops, was suspected on conventional enteroclysis in eight cases. On MRE, fibrofatty proliferation was disclosed in 15 cases, featuring as high-signal intensity, inhomogeneous fatty masses that were intersected by small mesenteric vascular branches of low signal intensity on true FISP images (Fig. 7).

Fig. 10 Coronal true FISP with fat saturation image (**a**) in a patient with Crohn's disease disclosed wall thickening and fissuring in a distal ileal loop. (**b**) Post-gadolinium 2D FLASH image reveals multi-layered enhancement pattern with hyperemic mucosa presenting with high signal intensity due to marked enhancement

Discussion

Despite the availability of many sensitive, direct or indirect techniques, small bowel imaging still remains a challenge. Advances in MRI hardware and software allow for the rapid acquisition of high-resolution images of the GI tract [3, 4]. MR enteroclysis (MRE) is an emerging technique for SB imaging, combining the advantages of cross-sectional imaging with those of volume challenge [6]. A most appealing quality of MRI is the lack of radiation exposure, an issue of paramount importance for young patients with Crohn's disease, who may need many such follow-up examinations. In addition, a variety of pulse sequences based on different contrast mechanisms may offer valuable information that can be integrated to provide a detailed view of the mucosal, mural and extramural abnormalities associated with the disease and complimentary information regarding disease activity and the presence of complications. Duodenal intubation renders MR enteroclysis less patient friendly [8, 9]. However, optimal luminal distension, achieved by MR enteroclysis, is currently considered to be a mandatory prerequisite to identify morphological changes induced by Crohn's disease confidently and to avoid misregistration [3, 10].

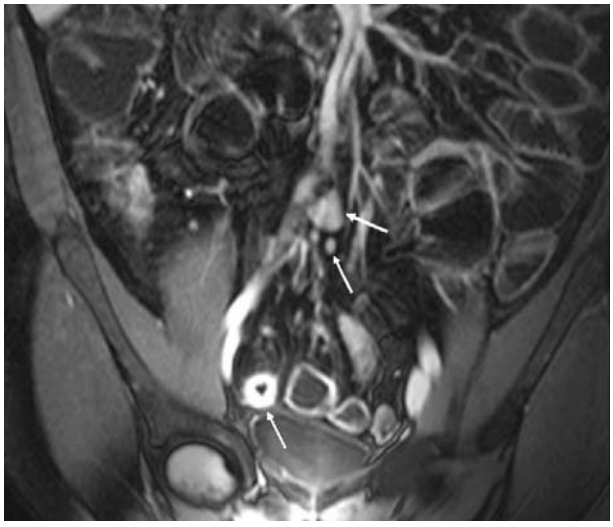

Fig. 11 Coronal post-gadolinium 2D FLASH image in a patient with Crohn's disease demonstrate marked transmural enhancement in a distal ileal loop (*dotted arrow*) and two enhancing mesenteric lymph nodes (*arrows*)

In the present study, MRE was found to be equal to conventional enteroclysis in detecting, localizing and estimating the length of all involved small bowel segments. Early lesions of Crohn's disease, such as thickening and distortion of the valvulae conniventes and superficial types of ulcers that were clearly demonstrated on CE were not consistently depicted by MRE. This resulted in an overall sensitivity of less than 50%, most probably due to inadequate spatial resolution. It is foreseen that dedicated ultrafast, high-resolution sequences and stronger gradients will further improve the detection of such early, but not specific, manifestations of the disease in the near future.

The characteristic discrete, longitudinal or transverse ulcers of Crohn's disease can be demonstrated on MRE, following optimal distension and homogeneous opacification of the bowel lumen. A sensitivity of about 90% in detecting deep ulcers was achieved, and this is probably related to the optimized technique that was utilized. However, in 2 out of 19 involved segments, deep ulcers were missed by MRE. Limited spatial resolution, as compared to CE, and/or partial volume effects due to the relatively thick slices acquired with MRE, may explain such results. Cobble-stoning, a combination of longitudinal and transverse ulceration, was easily shown by MRE. As in the case of discrete ulcers, a tailored MRE examination guaranteed a high sensitivity and specificity of 92.3 and 94.4%, respectively, for the demonstration of cobble-

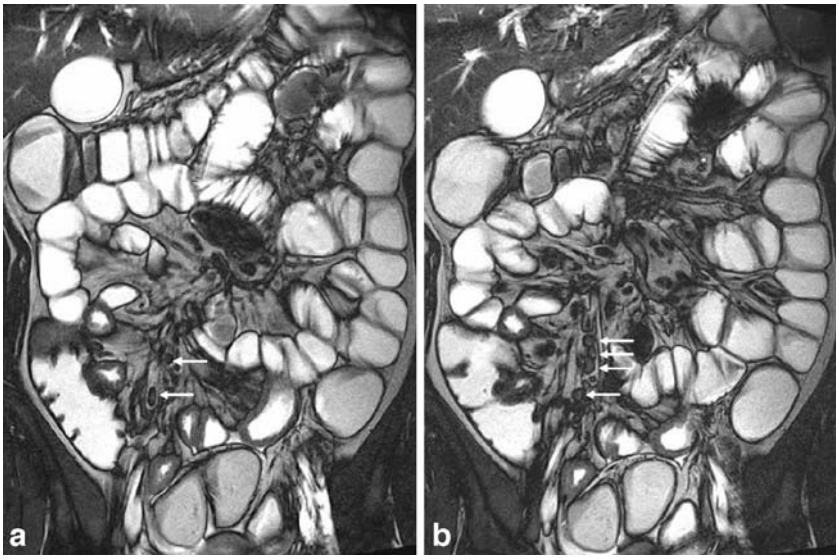

Fig. 12 Two consecutive coronal true FISP images on a patient with Crohn's disease demonstrating wall thickening and numerous small mesenteric lymph nodes

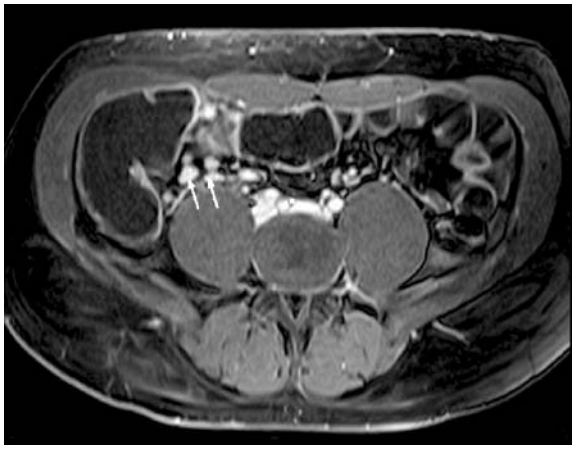

Fig. 13 Axial post-gadolinium 3D FLASH image on a patient with Crohn's disease disclosing at least three mesenteric lymph nodes exhibiting marked contrast enhancement

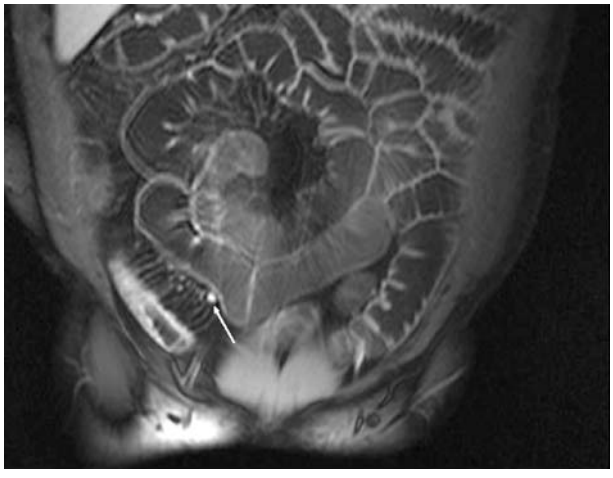

Fig. 14 Coronal post-gadolinium 2D FLASH image in a patient with Crohn's disease disclosing an involved ileal loop exhibiting marked enhancement. Mesenteric hypervascularity and a marked enhancing lymph node are also shown

stoning. A true FISP sequence is known to be superior to HASTE in demonstrating linear ulcers, cobble-stoning and intramural tracts, due to its superb resolution capabilities and its relative insensitivity to motion artifacts, while 3D FLASH sequences are less efficient in depicting such lesions when they are smaller than 3 mm [6]. Bowel wall thickening was clearly shown by all MRE sequences. Mural thickening presenting with moderate signal intensity on true FISP images was easily differentiated from misregistration due to the black boundary artifacts [4]. Bowel wall thickness and the length of small bowel involvement can be measured accurately on MRE images. Narrowing of the lumen and associated prestenotic dilatation, as well as skip or multiple lesions, were easily recognized on MRE images in all sequences. However, two false-positive cases with stenosis were diagnosed on MRE images, which were probably related to the inability of MRE to assess dynamically segmental motility effects and to rule out spasm. The development and application of dedicated pulse sequences offering fluoroscopic evaluation capabilities of stenotic segments might reduce the number of such false-positive results.

Exoenteric manifestations of the disease were demonstrated in detail on true FISP images due to the high contrast generated from the bright mesenteric fat. Complications such as fistulae, phlegmons or abscesses may be more accurately diagnosed on T1-weighted FLASH images with fat saturation by the characteristic pattern of enhancement after gadolinium administration [6]. The latter sequence is additionally useful in active disease because of the marked contrast uptake in the thickened SB wall [11, 12] and mesenteric lymph node enhancement [13]. As suggested by the current study and others, disease activity can be appreciated on MRE [11–15], and this may

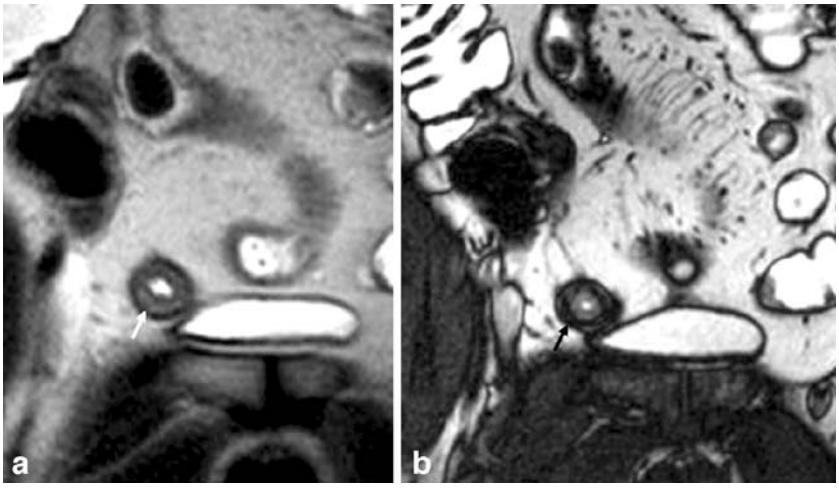

Fig. 15 Coronal HASTE (**a**) and true FISP (**b**) spot views in a patient with long-standing Crohn's disease. A submucosal layer with high signal intensity (*white arrow*) is depicted on HASTE image (**a**), which might correspond to the presence of edema or fat. True FISP image (**b**) can discriminate between the two by the characteristic black boundary artifact (*arrow*), which is exclusively due to the presence of intramural fat

represent one of the most important indications for the examination in the near future.

Intramural fat can be accurately identified when combining features from true FISP and gadolinium-enhanced 3D FLASH images with fat saturation. Discrimination between the deposition of fat and the presence of edema (Fig. 15) may be helpful for the disease classification. Collagen is known to result in late gadolinium enhancement [16]. In this context, MRE has the potential to differentiate fibrostenotic from edematous lesions on the basis of different gadolinium enhancement patterns.

MRE is an emerging technique for the assessment of small bowel pathology, and its clinical applications is so far limited to centers of reference. The present study shows that the method is complementary to CE in detecting superficial or early Crohn's disease, but it is of equal diagnostic accuracy in disclosing transmural disease. In addition, MRE can adequately depict mesenteric involvement and extraintestinal complications of Crohn's disease. Specific MRE imaging features may be used to assess disease activity. Furthermore, accurate individual lesion detection, provided by MRE, may successfully address clinical questions related to the classification of Crohn's disease subtypes.

References

1. Nolan DJ, Gourtsoyiannis NC (1980) Crohn's disease of the small intestine: a review of the radiological appearances in 100 consecutive patients examined by a barium infusion technique. Clin Radiol 31(5):597–603
2. Ruiz-Cruces R, Ruiz F, Perez-Martinez M, Lopez J, Tort Ausina I, de los Rios AD (2000) Patient dose from barium procedures. Br J Radiol 73(871): 752–761
3. Umschaden HW, Szolar D, Gasser J, Umschaden M, Haselbach H (2000) Small-bowel disease: comparison of MR enteroclysis images with conventional enteroclysis and surgical findings. Radiology 215:717–725
4. Gourtsoyiannis N, Papanikolaou N, Grammatikakis J, Maris T, Prassopoulos P (2000) Magnetic resonance imaging of the small bowel using a True-FISP sequence after enteroclysis with water solution. Invest Radiol 35(12):707–711
5. Gourtsoyiannis NC, Papanikolaou N, Grammatikakis J, Maris T, Prassopoulos P (2001) MR enteroclysis protocol optimization: comparison between 3d FLASH with fat saturation after intravenous gadolinium injection and true FISP sequences. Eur Radiol 11(6):908–913
6. Prassopoulos P, Papanikolaou N, Grammatikakis J, Rousomoustakaki M, Maris T, Gourtsoyiannis N (2001) MR enteroclysis imaging of crohn disease. Radiographics 21:161–172
7. Rofsky NM, Lee VS, Laub G, Pollack MA, Krinsky GA, Thomasson D, Ambrosino MM, Weinreb JC (1999) Abdominal MR imaging with a volumetric interpolated breath-hold examination. Radiology 212(3): 876–884
8. Narin B, Ajaj W, Gohde S et al (2004) Combined small and large bowel MR imaging in patients with Crohn's disease: a feasibility study. Eur Radiol 14:1535–1542
9. Lauenstein TC, Schneemann H, Vogt FM, Herborn CU, Ruhm SG, Debatin JF (2003) Optimization of oral contrast agents for MR imaging of the small bowel. Radiology 228:279–283
10. Gourtsoyiannis N, Papanikolaou N, Rieber A, et al (2002) Evaluation of the small intestine by MR imaging. In: Gourtsoyiannis N (ed) Radiological imaging of the small intestine. Springer, Berlin Heidelberg New York, pp 157–170
11. Schunk K, Kern A, Oberholzer K, Kalden P, Mayer I, Orth T, Wanitschke R (2000) Hydro-MRI in Crohn's disease. Appraisal of disease activity. Invest Radiol 35:431–437
12. Maccioni F, Viscido A, Broglia L, Marrollo M, Masciangelo R, Caprilli R, Rossi P (2000) Evaluation of Crohn's disease activity with magnetic resonance imaging. Abdom Imaging 25:219–228

13. Gourtsoyiannis N, Papanikolaou N, Grammatikakis J, Papamastorakis G, Prassopoulos P, Roussomoustakaki M (2004) Assessment of Crohn's disease activity in the small bowel with MR and conventional enteroclysis: preliminary results. Eur Radiol 14(6):1017–1024
14. Low RN, Sebrechts CP, Politoske DA, Bennett MT, Flores S, Snyder RJ, Pressman JH (2002) Crohn disease with endoscopic correlation: single-shot fast spin echo and gadolinium-enhanced fat-supressed spoiled gradient echo MR imaging. Radiology 222: 652–660
15. Koh DM, Miao Y, Chinn RJ et al (2001) MR Imaging evaluation of the activity in Crohn's disease. AJR 177:1325–1332
16. Semelka RC, Chung JJ, Hussain SM, Marcos HB, Woosley JT (2001) Chronic hepatitis: correlation of early patchy and late linear enhancement patterns on gadolinium-enhanced MR images with histopathology initial experience. J Magn Reson Imaging 13(3):385–391